ISBN: 978-3-95450-208-0 doi:10.18429/JACoW-IPAC2019-TUXXPLS3

THE DESIGN OPTIMIZATION OF THE DIELECTRIC ASSIST ACCELERATING STRUCTURE FOR BETTER HEAT AND GAS TRANSFER

Shingo Mori*, Mitsuhiro Yoshida†, KEK, Tsukuba, Japan
Daisuke Satoh‡, National Institute of Advanced Industrial Science and Technology, Tsukuba, Japan

Abstract

The dielectric-assist accelerating (DAA) structure is a dielectric-inserted normal-conducting cavity, which provides high Q value at room temperature. This accelerating structure is composed of dielectric disks and a dielectric cylindrical layer inserted in a copper cavity. For the realistic operation, the removal of heat from the dielectric cells and the vacuum evacuation of gas inside the cylindrical layers have not considered yet. In order to solve the problems, we propose the optimized design of the DAA structure, where the extended part of the dielectric disk is embedded in the copper cavity and the choke structure is applied. We show the result of the electromagnetic-field simulation of the extended DAA structure and the thermal simulation to clarify the relation between a duty factor and maximum temperature of the dielectric cells.

INTRODUCTION

A dielectric-assist accelerating (DAA) structure [1, 2] is promising in power efficiency and can be a new candidate of accelerating cavity for high duty operation because it provides high efficiency $Q \sim O(10^5)$ at room temperature, and higher Q value at low temperature. Although the DAA structure in the left figure of Fig. 1 has an advantage in efficiency, there are several problems required to consider before use of DAA cavity as an accelerator.

First, the thermal contact between the dielectric cell and the copper cavity is poor, because the dielectric cells and the copper cavity are not welded together. Since the volume heating of the dielectric cell is proportional to the square of the magnitude of the electric field inside the dielectric cell, poor thermal contact causes an overheating of the cells. A dielectric strength is known to be gradually decreasing at higher temperature. [3] Then the overheating of the dielectric cells may cause a breakdown at lower accelerating voltage.

Secondly, the pumping of gas from the inside of the DAA cavity is difficult in the original design. This is because some region in the left figure of Fig. 1 are enclosed between the dielectric cylinder and the copper cavity.

This paper is organized as follows. In Sec.2, we introduce optimized designs of the DAA cavity. In Sec.3, we will discuss the removal of heat from the dielectric disk. In Sec.5, we will conclude our results.

* smori@post.kek.jp
† mitsuhiro.yoshida@kek.jp
‡ dai-satou@aist.go.jp

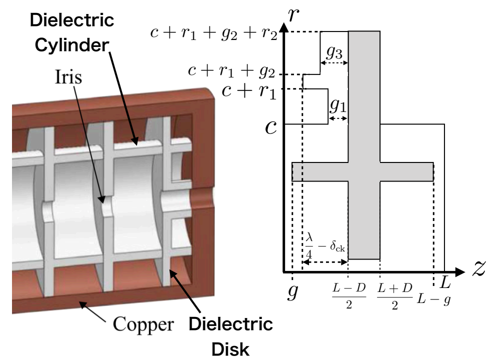

Figure 1: The original design of the test cavity with the DAA structure. (left) The definition of the parameters to distinguish the different choke structures. (right)

EXTENTION OF THE DAA STRUCTURE

An Extended Dielectric Disk and a Choke Structure

In order to remove heat from the cells, we consider enlarging the diameter of the dielectric disk so that the extended part of the disk is embedded in the copper cavity. Assuming good thermal contact, the larger contact area can mitigate overheating of the dielectric cells. In order to enhance heat conduction between them, we will apply metalization on the dielectrics and welding them together.

Since a radial transmission line has no cutoff frequency, all eigenmodes can leak via the extended disk. A solution with axial symmetry is to add a choke structure to the radial transmission line. [4, 5]

Comparison of Three Types of Extensions

In the application of the choke structure to the DAA structure, there are several ways. The first configuration shown in the left figure of Fig. 2 fills the choke structure with the dielectrics. The second one shown in the second figure from the left of Fig. 2 does not fill the choke structure with the dielectrics. The third one shown in the third figure from the left of Fig. 2 does not fill the choke structure with the dielectrics and has a vacuum region between the dielectric disk and the copper cylinder. The vacuum region enables the cavity to evacuate from the flank beside the beam holes.

The advantage of the first design named as type-1 is that a multipaction cannot happen in the choke structure. But it requires high accuracy of the machining of the dielectrics. Moreover, we need to care about the difference in the coeffi-

ISBN: 978-3-95450-208-0 doi:10.18429/JACoW-IPAC2019-TUXXPLS3

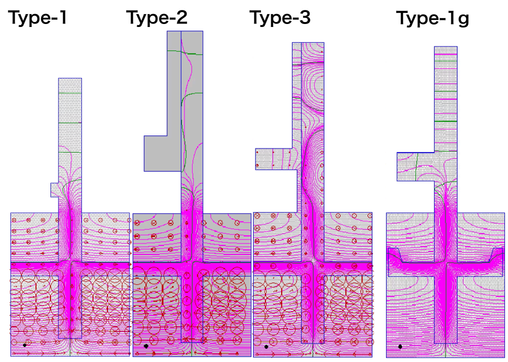

Figure 2: The choke application for the extended DAA structure. The horizontal line denotes the beam axis. We assume the axial symmetry of the structure and the field configuration. The red curves denote the real part of the electric force line and the green curves denote the imaginary part of that. The radius of the red circle denotes the magnitude of the axial component of the magnetic field.

cient of thermal expansion between the dielectrics and the copper. The temperature rises during the welding changes the radius of the choke part of the copper cavity and the dielectrics, which might crack the dielectrics if the bending strength of the dielectrics is low.

The second design named as type-2 has also high Q-value. The vacuum region in the choke structure requires a further considering of the multipaction and tests about a vacuum sealing between the dielectric disk and the copper cylinder.

In the third design named as type-3, we can enhance a pumping conductance by pumping from the end of the radial transmission line as well as the beam holes. But, in the radial transmission line and the choke structure, the vacuum region would cause the multipaction. Then the conditioning of the cavity would take longer hours than the previous two designs.

Optimization Using the Eigenmode Calculation

Tab. 1 shows the rf parameters and dimensions of the three designs shown in Fig. 2. In the right figure of Fig. 1, we show the definitions of the dimension parameters. In the obtained parameters listed in Tab. 1 and the eigenmode calculation described below, we use the parameter of polycrystalline magnesia applied in our previous paper [2]; the relative permitivity $\epsilon_r = 9.64$ and the loss tangent $\tan\delta = 6.0\times10^{-6}$ near 10 GHz.

We calculate the eigenmode of the accelerating mode for a single cell with a periodic-boundary condition through `SuperFish`. In the lattice of a parameter region of r_1, g_2, and δ_{ck} with number of the lattice points from 300 to 1000, we calculate the field configuration and the rf parameters such as Q-value and the shunt impedance. Using the obtained field configurations, we calculate the line integral of the magnetic field near the boundary between the dielectric disk and the copper cylinder, i.e.

$$I_{\rm rad} = \int_{c+r1}^{c+r1+r2+g2} drH|_{z=(L+D)/2-0}. \qquad (1)$$

We choose an optimized point from the data set generated above in the following steps. We select a dataset with higher Q-value of top 10%, then within them, we choose one data point which minimizes the value of $I_{\rm rad}$.

As at the junction of the radial transmission line and the choke structure the wall current vanishes, the accelerating mode does not transmit. Thus the simple design strategy is to minimize the wall current at the junction. In the right figure of Fig. 1 we show the definition of the dimension parameters used in the optimization process. The gray region denotes the dielectric cell and the white regions denote the vacuum. For the calculation of type-1, the length of choke structure, $\lambda/4-\delta_{\rm ck}$, is modified as $\lambda/(4n)-\delta_{\rm ck}$, where n is the refractive index of the dielectric material.

Table 1: Parameter List of Each Design

Name	type-1	type-2	type-3	type-1g
f_0 [MHz]	5711.2	5711.5	5711.4	5711.2
Q [10^5]	1.44	1.44	1.09	1.21
$Z_{\rm sh}$ [MV/m]	883	948	708	757
$I_{\rm rad}$ [A]	2.26	0.490	92.9	0.175
r_1 [mm]	5.0	12	12	9.0
r_2 [mm]	30	30	30	30
g_1 [mm]	–	–	1.0	–
g_2 [mm]	6.0	10	6.0	8.0
g_3 [mm]	–	3.0	2.0	–
$\delta_{\rm ck}$ [mm]	-1.0	5.0	3.0	-4.0
g [mm]	–	–	–	1.0

As we choose the larger gap between the dielectric disk and the copper cavity, g_1, the Q-value of the type-3 design, Q_3, decreases. From the calculation with `SuperFish` we obtain a relation $Q_3(g_1) = Q_{0,3}(1-\alpha g_1)$, where α is the dimensionful parameter to quantify the reduction of the Q-value of type-3 design per 1[mm] of the gap, g_1. We obtained $\alpha = 0.20$.

A Gap Between the Cylindrical Layer

In the original DAA structure shown in the left figure of Fig. 1 and the design of type-1 and type-2 in Fig. 2, the evacuation is still difficult in the region enclosed by the dielectric cylinder and the copper cavity.

In the above designs, the copper cylinder fixes the position of the dielectric disks. In the design of type-1 and type-2, the copper cylinder sandwiches the extended part of the dielectric disk, and then fixes the position of the dielectric disk. In type-3, the dielectric cylinder can be welded together with the copper cylinder.

Thus, we can disconnect neighboring dielectric cells and give a gap between the cells as shown in the right figure of Fig. 2 named as type-1g. The gap makes the entire vacuum region connected, which provides an ability to evacuate

ISBN: 978-3-95450-208-0 doi:10.18429/JACoW-IPAC2019-TUXXPLS3

whole the vacuum region from the beam hole for the three design proposed above.

We numerically calculate a relation between the Q-value of the type-1 design, $Q_{0,1}$ and one of the type-1g with a gap 2g [mm] between two neighboring cells, $Q_1(g) = Q_{0,1}(1 - \alpha' g)$, where α' is the dimensionful fitted parameter. We obtained $\alpha' = 0.16$.

THE THERMAL TRANSFER FROM THE DIELECTRIC CELLS TO THE COPPER

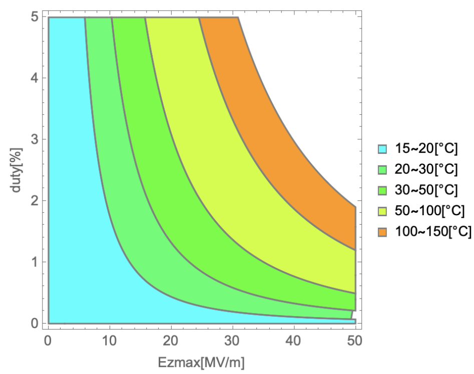

Figure 3: The maximum temperature of the dielectric cell for various duty factors and accelerating voltages.

Fig. 3 shows the relation among the maximum temperature of the dielectric cell and the accelerating voltage and the duty factor for the type-1 cavity, which is obtained as explained below. The volume loss in the dielectric cell is proportional to square of the accelerating voltage and linearly proportional to the duty factor and the maximum temperature. We determine the maximum temperature of the dielectric cell by the transient thermal solver of CST, where we fix the circumference temperature of the cavity at 15°C. Then we obtain a relation between the the maximum temperature of the dielectric cell, $T_{\rm max}$ [°C], and the volume loss corresponding to the maximum accelerating gradient $E_{\rm acc,max}$ [MV/m] with duty factor as $r_{\rm duty}$ [%],

$$T_{\rm max} = T_0 + k\frac{r_{\rm duty}}{100}E^2_{\rm acc,max}, \quad (2)$$

where the ambient temperature $T_0 = 15.0$ [°C] and the fitted dimensionful parameter $k = 0.0284$.

In the above calculation, we assume the perfect thermal contact between the copper and the dielectric cells of MgO. As long as we can guarantee the perfect thermal contact, the situation is not different in the other two types of designs.

DISCUSSION AND CONCLUSION

The DAA structure is a candidate for the high duty accelerator at room temperature. Still, the actual use of the DAA cavity as an accelerator component has several requirements. We propose three candidates of solutions to solve the problems.

First, the thermal transfer from the dielectric cells to the copper cavity is required to avoid the overheating of the cells. To solve the problem, we make the extended dielectric disk embedded in the copper cavity, so that the contact area increases as shown in the four designs in Fig. 2. This prescription has a side effect, which enables the copper cavity to fix the position of the dielectric cells without stacking the cells touching with each other as the type-1g.

Secondly, the original DAA structure has a closed region which is between the copper cavity and the dielectric cell, where we can not pump easily from those regions. The designs of type-3 and type-1g can solve this problem. While Type-3 requires both the side hole of the cavity and the beam hole to evacuate, type-1g can be evacuated only from the beam hole. Moreover, for the same separation of the gap, g_1 for type-3 and 2g for type-1g, type-1g has higher Q-value than that of type-3.

As future works, we will consider the effects of the multipaction and the wakefield. In the design of type-2, type-3 and type-1g, the narrow gaps and the high secondary-electron yeild of the dielectrics will cause a multipactoring at some input power depending on the dimension of the gaps. The dumping of wakefields produced by the transverse beam offset is also important for the high current accelerator.

ACKNOWLEDGEMENTS

This work is supported by JSPS KAKENHI Grant No. 16H02134. The authors would like to thank N. Shigeoka from the Mitsubishi Heavy Industries Mechatronics Systems Ltd. for their continued support of the development of DAA structures.

REFERENCES

[1] D. Satoh, M. Yoshida, and N. Hayashizaki, "Dielectric assist accelerating structure", *Physical Review Accelerators and Beams*, vol. 19, no. 1, p. 011 302, 2016.

[2] D. Satoh, M. Yoshida, and N. Hayashizaki, "Fabrication and cold test of dielectric assist accelerating structure", *Physical Review Accelerators and Beams*, vol. 20, no. 9, p. 091 302, 2017.

[3] Y. Q. Wu, H. C. Lin, P. D. Ye, and G. D. Wilk, "Current transport and maximum dielectric strength of atomic-layer-deposited ultrathin al 2 o 3 on gaas", *Applied physics letters*, vol. 90, no. 7, p. 072 105, 2007.

[4] T. Shintake, "The choke mode cavity", *Japanese Journal of Applied Physics*, vol. 31, no. 11A, p. L1567, 1992.

[5] H. Zha *et al.*, "Choke-mode damped structure design for the compact linear collider main linac", *Physical Review Special Topics-Accelerators and Beams*, vol. 15, no. 12, p. 122 003, 2012.